

Influence of strain on the electronic structure of the TbMnO₃/SrTiO₃ epitaxial interface

S. Venkatesan, M. Döblinger, C. Daumont, B. Kooi, B. Noheda et al.

Citation: *Appl. Phys. Lett.* **99**, 222902 (2011); doi: 10.1063/1.3663218

View online: <http://dx.doi.org/10.1063/1.3663218>

View Table of Contents: <http://apl.aip.org/resource/1/APPLAB/v99/i22>

Published by the [AIP Publishing LLC](#).

Additional information on *Appl. Phys. Lett.*

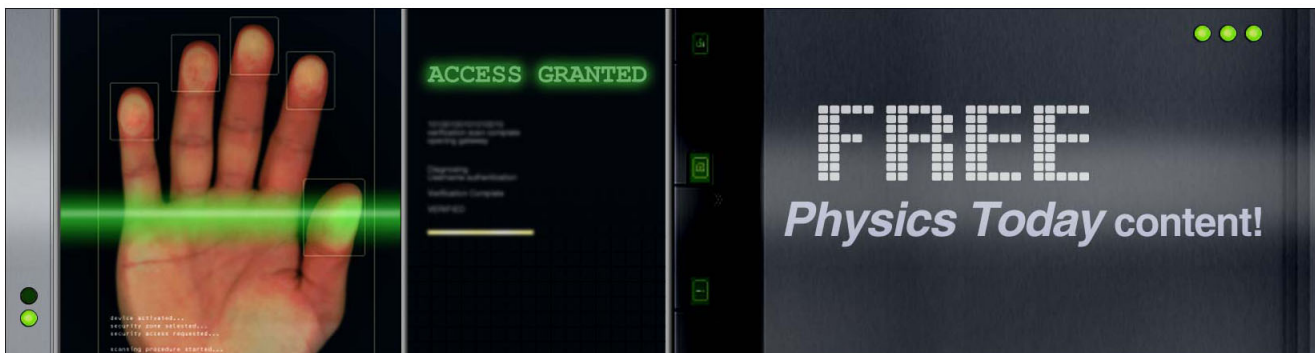
Journal Homepage: <http://apl.aip.org/>

Journal Information: http://apl.aip.org/about/about_the_journal

Top downloads: http://apl.aip.org/features/most_downloaded

Information for Authors: <http://apl.aip.org/authors>

ADVERTISEMENT



Influence of strain on the electronic structure of the TbMnO₃/SrTiO₃ epitaxial interface

S. Venkatesan,^{1,a)} M. Döblinger,¹ C. Daumont,² B. Kooi,² B. Noheda,² J. T. M. De Hosson,² and C. Scheu^{1,b)}

¹Department of Chemistry and Center for NanoScience, Ludwig-Maximilians-Universität München, Butenandstr 5-13(E), 81377 München, Germany

²Zernike Institute for Advanced Materials, University of Groningen, Nijenborgh 4, 9747 AG Groningen, The Netherlands

(Received 16 September 2011; accepted 29 October 2011; published online 29 November 2011)

Understanding the magnetotransport properties of epitaxial strained thin films requires knowledge of the chemistry at the interface. We report on the change in Mn electronic structure at the epitaxially strained TbMnO₃/SrTiO₃ interface. Scanning transmission electron microscopy shows an abrupt interface with a bright contrast, indicating the presence of misfit strain. Electron energy loss spectroscopy displays a chemical shift of the Mn L_{2,3} edge together with a high white line intensity ratio revealing a reduction in the nominal Mn oxidation state in the first 3–4 monolayers. These observations indicate misfit strain significantly changes the electronic structure at the interface. © 2011 American Institute of Physics. [doi:10.1063/1.3663218]

The coupling between magnetic and ferroelectric order parameters in so-called magnetoelectric multiferroics has drawn considerable interest due to their potential application as multifunctional devices.^{1–3} Among perovskite manganite based multiferroics, orthorhombic TbMnO₃ (TMO) has a prominent place because of its large magnetoelectric coupling and since its ferroelectric state is directly coupled to the magnetic structure.^{4,5} Epitaxially stabilized thin films offer the possibility of utilizing the misfit strain to have additional degrees of freedom for tuning the properties.⁶ In a recent development, epitaxial TMO films grown on SrTiO₃ (STO) substrates exhibit net magnetic moments.^{7–9} The proposed origin for the net magnetic moments in this system has been attributed to epitaxial strain-induced unit cell deformation,⁸ leading to the changes in their magnetic interaction. Detailed investigation on growth, structure, transport properties and thickness dependent domain structure of the epitaxial TMO films have been reported elsewhere.^{10,11} Nonetheless, there is to-date a lack of detailed investigation on interfacial strain, chemistry, and electronic structure of the TMO/STO epitaxial interface. In this letter, we address these questions by using scanning transmission electron microscopy (STEM) based techniques, such as high angle annular dark field (HAADF) imaging and electron energy loss spectroscopy (EELS) at the sub nanometer scale.

The details of the growth of orthorhombic (001)-oriented TMO films on (001)-STO substrates were discussed by Daumont *et al.*,¹⁰ and in this present work, a 67 nm thick TMO film was investigated. Cross section TEM samples were prepared by a conventional procedure as described in detail elsewhere¹¹ and plasma cleaned before loading the sample into the microscope. Interface structure characterization and chemical analysis were carried out using a FEI Titan 80-300 TEM/STEM field emission TEM operating at 300 kV, equipped with a Gatan Tridiem imaging filter. The

probe size used for EELS, annular dark field (ADF), and HAADF imaging was 2 Å taking beam broadening into consideration. EEL spectra were acquired with a convergence semiangle of 9.5 mrad and a collection angle of about 12 mrad at dispersions of 0.1, 0.2, and 0.3 eV/channel in order to obtain data with high energy resolution and good signal to noise ratio. All data shown were acquired with a dispersion of 0.2 eV/channel. A spectrometer entrance aperture of 2 mm was used, resulting in an energy resolution of about 1 eV as determined by the full width at half maximum of the zero loss peak. Core-loss EEL spectra at the Mn L_{2,3}, O K, Ti L_{2,3}, and Tb M_{4,5} edges were recorded over an area of (2 × 0.6) nm² as a function of probe-interface distance. Care was taken such that the long side of the probed rectangular regions was aligned parallel to the interface to obtain high lateral resolution perpendicular to the interface. Using an elongated box for measurements allows to minimize beam damage and to correct for the specimen drift.

Bulk TMO has an orthorhombic structure (space group Pbnm) with lattice parameters $a = 5.2931$ Å, $b = 5.8384$ Å, $c = 7.4025$ Å at room temperature.¹² Our earlier x-ray data have shown that the film is compressively strained for the present thickness and adopts two different orientation relationships with the underlying STO substrate, i.e., [100] and [010] of the orthorhombic TMO film parallel to the [110] and [1 $\bar{1}$ 0] of the cubic substrate. With this orientation relationship the strain is only partially relaxed.¹⁰ Assuming full coherency between TMO and STO, the misfit strain is as large as 4.1% and –5.7% for an orientation relationship of a axis TMO//STO [110] and b axis TMO//STO [1 $\bar{1}$ 0], respectively. Even for the high thickness of 67 nm, the film remains in the strained state. The overview of the TMO film on STO is shown in a low magnification HAADF-STEM image in Fig. 1(a). The intensity in the HAADF image is approximately proportional to the average atomic number Z^2 of the projected atomic columns. Since the average atomic number of the TMO film is higher than that of STO, TMO appears brighter. The interface between film and substrate appears

^{a)}Electronic mail: sriram.venkatesan@cup.uni-muenchen.de.

^{b)}Electronic mail: christina.scheu@cup.uni-muenchen.de.

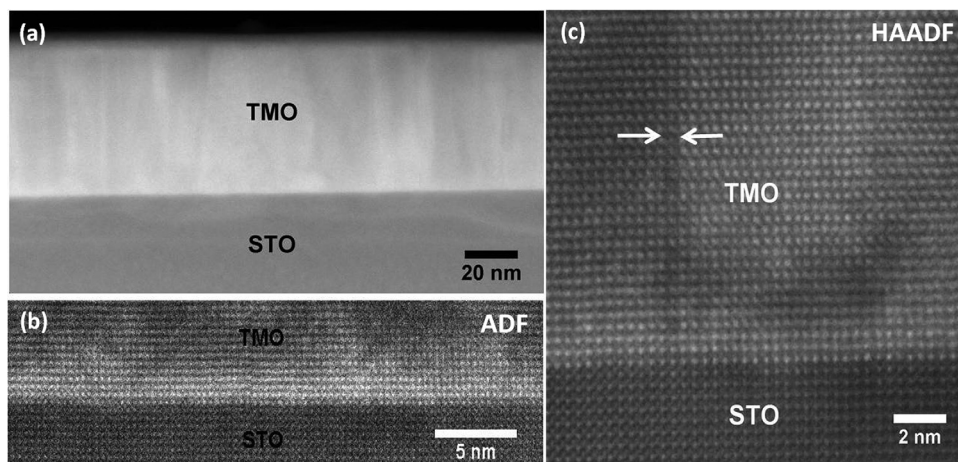


FIG. 1. Cross section view of (a) low magnification HAADF-STEM image of the TMO film on STO substrate, (b) an overview of low angle ADF image revealing strain contrast at the TMO/STO interface region, and (c) high resolution HAADF-STEM image (noise filtered) showing an atomically coherent TMO/STO interface. The arrows indicate a domain wall.

relatively abrupt and coherent without any interfacial defect or misfit dislocations (see Fig. 1(c)). An interesting feature is observed at the substrate-film interface in the high resolution HAADF-STEM image of Fig. 1(c) collected with a detector inner semiangle of 59 mrad. The domain boundaries/walls formed as a part of strain relaxation mechanism have a standoff of about 1.5 nm above the interface. In Fig. 1(b), the low angle ADF image collected with a detector inner semiangle of 30 mrad is given, which reveals an enhanced bright band near the interface with a width of about 1.5 nm. When the electron beam probes across the interface, the atoms displaced from the crystal symmetry positions (due to strain or by lattice vibrations) cause disruption in the channeling of the incident scanning beam. This dechanneling affects the fast electron scattering through large angles.^{13,14} As a result, the ADF intensity collected from the strained region is higher than that from the strain free region as seen in Fig. 1(b). This is consistent with cross section bright field TEM image of the same film¹¹ showing strain fields at the substrate-film interface and the reduced in-plane lattices a , b found in our x-ray diffraction data.¹⁰ Thus, both features, the stand off of the domain walls and the enhanced low angle ADF signal, suggest that the interface is strained compared to the bulk region.

An atomically abrupt interface does not necessarily imply that the atom possesses the same valence state as in the bulk. To obtain information on the electronic structure of the TMO/STO interface, EEL spectra were recorded across the interface from the substrate to the film with 0.6 nm steps parallel to the interface with the settings previously mentioned. The background was subtracted using a power law fit.¹⁵ Noticeable strong changes were observed at the Mn $L_{2,3}$ edge which will be therefore discussed in detail. Fig. 2 shows the Mn $L_{2,3}$ ionization edge around 640 eV as the function of probe-interface distance. The Mn edge typically shows two characteristic L_3 and L_2 white lines (WL) with an energy loss difference of ~ 11 eV due to spin-orbit splitting. The peak arises due to transitions of electrons from the $2p_{3/2}$ and $2p_{1/2}$ core levels to empty manganese 3d states hybridized with oxygen 2p orbitals.¹⁶ The WL intensity ratio is sensitive to the d electron occupancy in 3d transition metal and oxides,¹⁷ and it can serve as a useful finger print for the valence state at the interface.^{18–21} For Mn, we rely on the

data from Schmidt *et al.*²² The continuum contribution of the WL intensity was approximated by a Hartree-Slater cross-section step function and removed from the original data. Fig. 2 shows that the Mn edge starts from the interface region. When the EELS data are acquired at the interface positions 0, 1, and 2 as marked in the figure, the Mn $L_{2,3}$ edge onset shifts towards lower energy losses in comparison with the spectrum collected at the position 4 at a distance of 5 nm away from the interface (bulk region). Fitting a double Gaussian to the L_3 peak for the spectra acquired at a bulk region and at position 1 of the interface region reveals that

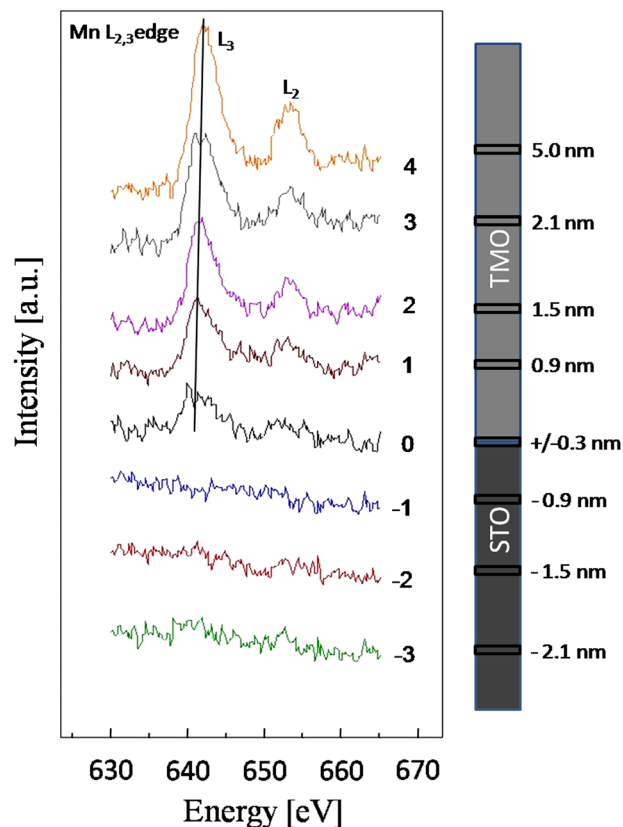


FIG. 2. (Color online) EEL spectra across the interface between STO and TMO showing the variation in the Mn $L_{2,3}$ edge with two characteristic peaks labeled as L_3 and L_2 . The line drawn in the Mn L_3 edge is a guide to eye to see the shift in the edges. All the spectra were displaced vertically for the sake of clarity.

this peak shifts by 0.7 eV. The peak maxima of L_3 at the interface is at 641.3 eV (± 0.2) and the L_3/L_2 intensity ratios calculated from the spectra acquired at the interface region (position 0 and 1) measures $3.1(\pm 0.3)$ and $2.7(\pm 0.3)$, respectively. The intensity ratios obtained above 0.9 nm from the interface at the positions 2, 3, and bulk region are $2.6(\pm 0.2)$, $2.5(\pm 0.2)$, and $2.5(\pm 0.2)$, respectively, which is consistent with previous reports for Mn in 3+ oxidation state.²² A striking feature is that the largest $I(L_3)/I(L_2)$ ratio is observed only at the interface region where the high strain contrast is seen in the low angle ADF-STEM image (Fig. 1(b)). The WL intensity ratios are known to increase with decreasing transition-metal valencies for the transition metal oxides.²³ In our case, the high intensity ratio at the interface can be correlated to Mn atoms in lower oxidation state compared to the bulk. Each of the changes seen in the Mn $L_{2,3}$ edge while moving the probe across the TMO interface region into the bulk TMO can be related directly to a corresponding change in the local electronic structure. In a purely ionic picture, the combination of a weak chemical shift and a higher WL ratio would indicate a tendency towards a slight reduction in the Mn oxidation state locally at the interface region. It is known that this is not the case in transition metal oxides,²⁴ where these features are better interpreted as changes in local charge transfer. Nevertheless, our results are consistent with those obtained for the Mn K edges of TMO thin films⁷ and of bulk TMO under hydrostatic pressure²⁵ and can be interpreted as an increase in the ionicity and/or a decrease of the local Jahn-Teller distortion.^{7,25} X-ray photoelectron spectroscopy data in similar films (measured at the free surface)⁷ revealed similar features at the Mn K edge but not at the Mn L edge, as in the present work, which indicates that the effect is greatly amplified at the strained interface.

In conclusion, our work demonstrates the change in electronic structure at the interface of TMO/STO due to misfit strain using HAADF, ADF and EELS. The high resolution HAADF-STEM image infers that the domain walls have a stand off about 1.5 nm above the interface and that the interface is coherent and fairly abrupt. A clear uniform strain contrast is visible for a width of about 1.5 nm from the interface in the high resolution low angle ADF-STEM images. The observed compressively strained layers are responsible for the evolution of a weak chemical shift in the Mn $L_{2,3}$ edge towards lower energy losses. Together with the higher WL intensity ratio calculated at the interface, a slight change of the local charge distribution is evident. Finally, this finding

opens the possibility to control the electronic structure at the interface by tuning the epitaxial misfit strain.

Authors S.V, M.D, and C.S would like to acknowledge Dr. Steffen Schmidt for his help in microscope operation and useful discussion. C.S would like to thank the German research foundation (DFG) for funding in the Cluster of Excellence "Nanosystems Initiative Munich" (NIM).

¹N. Hur, S. Park, P. Sharma, S. Ahn, S. Guha, and S. Cheong, *Nature (London)* **429**, 392 (2004).

²M. Fiebig, *J. Phys. D* **38**, R123 (2005).

³W. Eerenstein, N. D. Mathur, and J. F. Scott, *Nature (London)* **442**, 759 (2006).

⁴M. Kenzelmann, A. B. Harris, S. Jonas, C. Broholm, J. Schefer, S. B. Kim, C. L. Zhang, S. Cheong, O. P. Vajk, and J. W. Lynn, *Phys. Rev. Lett.* **95**, 087206 (2005).

⁵M. Mostovoy, *Phys. Rev. Lett.* **96**, 067601 (2006).

⁶P. Zubko, S. Gariglio, M. Gabay, P. Ghosez, and J. Triscone, *Annu. Rev. Condens. Matter Phys.* **2**, 14165 (2011).

⁷D. Rubi, C. de Graaf, C. J. M. Daumont, D. Mannix, R. Broer, and B. Noheda, *Phys. Rev. B* **79**, 014416 (2009).

⁸X. Marti, V. Skumryev, A. Cattoni, R. Bertacco, V. Laukhin, C. Ferrater, M. V. Garcia-Cuenca, M. Varela, F. Sanchez, and J. Fontcuberta, *J. Magn. Magn. Mater.* **321**, 1719 (2009).

⁹B. J. Kirby, D. Kan, A. Luykx, M. Murakami, D. Kundaliya, and I. Takeuchi, *J. Appl. Phys.* **105**, 07D917 (2009).

¹⁰C. J. M. Daumont, D. Mannix, S. Venkatesan, G. Catalan, D. Rubi, B. J. Kooi, J. T. M. D. Hosson, and B. Noheda, *J. Phys: Condens. Matter.* **21**, 182001 (2009).

¹¹S. Venkatesan, C. Daumont, B. J. Kooi, B. Noheda, and J. T. M. D. Hosson, *Phys. Rev. B* **80**, 214111 (2009).

¹²J. A. Alonso, M. J. Martinez-Lopez, and M. T. Casais, *Inorg. Chem.* **39**, 917 (2000).

¹³Z. Yu, D. A. Muller, and J. Silcox, *J. Appl. Phys.* **95**, 3362 (2004).

¹⁴A. T. J. van Helvoort, Ø. Dahl, B. G. Soleim, R. Holmestad, and T. Tybell, *App. Phys. Lett.* **86**, 092907 (2005).

¹⁵R. F. Egerton, *Electron Energy Loss Spectroscopy in the Electron Microscope*, 2nd ed. (Plenum, New York, 1996).

¹⁶H. Kurata and C. Colliex, *Phys. Rev. B* **48**, 2102 (1993).

¹⁷R. D. Leapman, L. A. Grunes, and P. L. Fejes, *Phys. Rev. B* **26**, 614 (1982).

¹⁸D. Loomer, T. Al, L. Weaver, and S. Cogswell, *Am. Mineral.* **92**, 72 (2007).

¹⁹S. Zhang, K. J. T. Livi, A. C. Gaillot, A. T. Stone, and D. R. Veblen, *Am. Mineral.* **95**, 1741 (2010).

²⁰T. Riedl, T. Gemming, and K. Wetzig, *Ultramicroscopy* **106**, 284 (2006).

²¹J.-L. Maurice, F. Pailloux, D. Imhoff, N. Bonnet, L. Samet, A. Barthelémy, J.-P. Contour, C. Colliex, and A. Fert, *Eur. Phys. J. Appl. Phys.* **24**, 215221 (2003).

²²H. K. Schmidt and W. Mader, *Micron* **37**, 426 (2006).

²³J. H. Rask, B. A. Miner, and P. R. Buseck, *Ultramicroscopy* **21**, 321 (1987).

²⁴H. Raebiger, S. Lany, and A. Zunger, *Nature (London)* **453**, 763 (2008).

²⁵J. M. Chen, T. L. Chou, J. M. Lee, S. A. Chen, T. S. Chan, T. H. Chen, K. T. Lu, W. T. Chuang, H.-S. Sheu, and S. W. Chen *et al.*, *Phys. Rev. B.* **79**, 165110 (2009).